A Dimeric FAP-Targeting Small-Molecule Radioconjugate with High and Prolonged Tumor Uptake

Andrea Galbiati*[1], Aureliano Zana*[1], Matilde Bocci[1], Jacopo Millul[1], Abdullah Elsayed[1,2], Jacqueline Mock[1], Dario Neri[2,3], and Samuele Cazzamalli[1]

[1]*Research and Development Department, Philochem AG, Otelfingen, Switzerland;* [2]*Department of Chemistry and Applied Biosciences, Swiss Federal Institute of Technology, Zurich, Switzerland; and* [3]*Philogen S.p.A., Siena, Italy*

Imaging procedures based on small-molecule radioconjugates targeting fibroblast activation protein (FAP) have recently emerged as a powerful tool for the diagnosis of a wide variety of tumors. However, the therapeutic potential of radiolabeled FAP-targeting agents is limited by their short residence time in neoplastic lesions. In this work, we present the development and in vivo characterization of BiOncoFAP, a new dimeric FAP-binding motif with an extended tumor residence time and favorable tumor-to-organ ratio. **Methods:** The binding properties of BiOncoFAP and its monovalent OncoFAP analog were assayed against recombinant human FAP. Preclinical experiments with ^{177}Lu-OncoFAP-DOTAGA (^{177}Lu-OncoFAP) and ^{177}Lu-BiOncoFAP-DOTAGA (^{177}Lu-BiOncoFAP) were performed on mice bearing FAP-positive HT-1080 tumors. **Results:** OncoFAP and BiOncoFAP displayed comparable subnanomolar dissociation constants toward recombinant human FAP in solution, but the bivalent BiOncoFAP bound more avidly to the target immobilized on solid supports. In a comparative biodistribution study, ^{177}Lu-BiOncoFAP exhibited a more stable and prolonged tumor uptake than ^{177}Lu-OncoFAP (~20 vs. ~4 percentage injected dose/g, respectively, at 24 h after injection). Notably, ^{177}Lu-BiOncoFAP showed favorable tumor-to-organ ratios with low kidney uptake. Both ^{177}Lu-OncoFAP and ^{177}Lu-BiOncoFAP displayed potent antitumor efficacy when administered at therapeutic doses to tumor-bearing mice. **Conclusion:** ^{177}Lu-BiOncoFAP is a promising candidate for radioligand therapy of cancer, with favorable in vivo tumor-to-organ ratios, a long tumor residence time, and potent anticancer efficacy.

Key Words: fibroblast activation protein; theranostics; OncoFAP; targeted radiotherapy; dimeric targeting ligands

J Nucl Med 2022; 63:1852–1858
DOI: 10.2967/jnumed.122.264036

Small-molecule radioconjugates (SMRCs) are pharmaceutical products comprising a small organic ligand that acts as a tumor-targeting agent and a radionuclide payload that can be exploited for both diagnostic and therapeutic applications (*1–3*). The theranostic potential of SMRCs—that is, the possibility to perform imaging and therapy with the same product—facilitates the clinical development of this new class of drugs (*4–7*). Patients who can predictably benefit from targeted radioligand therapy are accurately selected through dosimetry studies (*8*). ^{177}Lu-DOTATATE (Lutathera; Advanced Accelerator Applications), a radioligand therapeutic targeting somatostatin receptor type 2, is the first SMRC product that gained marketing authorization for therapy of neuroendocrine tumors (*9*). The use of this drug has consistently shown high response rates and long median progression-free survival in a multicenter phase III clinical trial (*10*). More recently, a second product, named ^{177}Lu-PSMA-617, was shown to provide therapeutic benefit to PSMA-positive metastatic castration-resistant prostate cancer patients in a large phase III clinical trial (*11*). Radioligand therapy with ^{177}Lu-PSMA-617 prolonged imaging-based progression-free survival and overall survival when added to standard care (*11*).

In the last few years, a new category of pan-tumoral tumor-targeting SMRCs specific to fibroblast activation protein (FAP) has been successfully implemented for the diagnosis of solid tumors (*12–15*). FAP is a membrane-bound enzyme highly expressed on the surface of cancer-associated fibroblasts in the stroma of more than 90% of human epithelial cancers. FAP expression in healthy tissues is negligible (*12,13,16,17*). We have recently reported the discovery of OncoFAP, the small-molecule FAP-targeting agent with the highest affinity reported so far (*18*). Proof-of-concept targeting studies with ^{68}Ga-OncoFAP-DOTAGA (^{68}Ga-OncoFAP), a PET tracer based on OncoFAP, have confirmed excellent biodistribution in patients with different primary and metastatic solid malignancies (*19*).

The efficacy of radioligand therapeutics correlated strongly with their residence time in tumors (*9,20–23*). Although ^{177}Lu-DOTATATE and PSMA-617 are characterized by a sustained tumor residence time in patients (i.e., ~61 h for ^{177}Lu-PSMA-617 and ~88 h for ^{177}Lu-DOTATATE) (*24,25*), SMRCs based on FAP-targeting agents are typically cleared from solid lesions in a few hours (*26,27*). In preclinical biodistribution experiments, ^{177}Lu-OncoFAP selectively localized on neoplastic lesions (~38 percentage injected dose [%ID]/g 1 h after systemic administration), but half the dose delivered to the tumor was lost within 8–12 h (*18*). A comparable tumor-targeting performance and pharmacokinetic profile have been reported for other FAP-targeting SMRCs by Loktev et al. (e.g., the tumor uptake of ^{177}Lu-FAPI-46 decreased from 12.5 %ID/g at 1 h to 2.5 %ID/g at 24 h after administration) (*28*). Importantly, a rapid washout from tumors was observed not only in mice but also in patients treated with ^{177}Lu-FAPI-46 (*26,29*).

In an attempt to extend the tumor residence time of FAP-targeting SMRCs and to maximize the exposure of cancer cells to biocidal radiation, we developed BiOncoFAP, a dimeric FAP-targeting OncoFAP derivative. In this work, we describe the in vitro characterization of BiOncoFAP and we report the first preclinical biodistribution and therapy studies with a radiolabeled preparation of this novel dimeric FAP-targeting compound.

Received Feb. 21, 2022; revision accepted May 10, 2022.
For correspondence or reprints, contact Samuele Cazzamalli (samuele.cazzamalli@philochem.ch) or Dario Neri (neri@pharma.ethz.ch).
*Contributed equally to this work.
Published online May 19, 2022.

MATERIALS AND METHODS

Chemistry and Radiochemistry

(*S*)-4-((4-((2-(2-cyano-4,4-difluoropyrrolidin-1-yl)-2-oxoethyl)carbamoyl)quinolin-8-yl)amino)-4-oxobutanoic acid (named OncoFAP-COOH), OncoFAP-fluorescein, OncoFAP-Alexa488, and OncoFAP-IRDye750 were synthesized as previously reported by Millul et al. (*18*). OncoFAP-DOTAGA (compound 1) and BiOncoFAP-DOTAGA (compound 4) were labeled with cold lutetium by incubation with [^{nat}Lu]$LuCl_3$ in acetate buffer at 90°C for 15 min to obtain ^{nat}Lu-OncoFAP-DOTAGA (compound 2) and ^{nat}Lu-BiOncoFAP-DOTAGA (compound 5), which were used as reference compounds for in vitro characterization (inhibition assay and serum stability). The structures of OncoFAP and BiOncoFAP conjugates are depicted in Figure 1. Detailed experimental chemical procedures are described in the supplemental material (available at http://jnm.snmjournals.org).

OncoFAP-DOTAGA (compound 1) and BiOncoFAP-DOTAGA (compound 4) were radiolabeled with ^{177}Lu using different specific activities for the different studies (biodistribution and therapy). Before the biodistribution study, precursors (compound 1 or 4, 100 nmol) were dissolved in 100 μL of phosphate-buffered saline (PBS) and diluted with 200 μL of sodium acetate (1 M in water, pH 8). Twenty megabecquerels of ^{177}Lu solution were added, and the mixture was heated at 90°C for 15 min, followed by dilution with 1,600 μL of PBS to achieve a final volume of 2 mL. Before the therapy studies, precursors (compound 1 or 4, 5 nmol) were dissolved in 5 μL of PBS, and then sodium acetate buffer (30 μL, 1 M in water) and 15 or 70 MBq of ^{177}Lu solution were added. The mixture was heated at 90°C for 15 min, followed by dilution with 130 μL of PBS to afford a final volume of 200 μL. Quality control of the radiosynthesis was performed using radio-high-performance liquid chromatography. The possibility of forming a stable complex between the so-obtained ^{177}Lu-radiolabeled derivatives and the target antigen was tested by coincubating the compounds with recombinant human FAP (hFAP) and loading the mixture onto a desalting PD-10 column run by gravity (Supplemental Fig. 1).

In Vitro Inhibition Assay on hFAP

The enzymatic activity of hFAP on the Z-Gly-Pro-AMC substrate was measured at room temperature on a microtiter plate reader, monitoring the fluorescence at an excitation wavelength of 360 nm and an emission wavelength of 465 nm. The reaction mixture contained substrate (20 μM), protein (200 pM, constant), assay buffer (50 mM Tris, 100 mM NaCl, and 1 mM ethylenediaminetetraacetic acid, pH 7.4), and inhibitors (compounds 1, 2, 4, and 5) with serial dilution from 1.67 μM to 800 fM, 1:2 in a total volume of 20 μL. Experiments were performed in triplicate, and the mean fluorescence values were fitted using Prism, version 7 (GraphPad) [y = bottom + (top − bottom)/$(1 + 10^{((\mathrm{LogIC50} - X)*\mathrm{HillSlope})})$]. The value is defined as the concentration of inhibitor required to reduce the enzyme activity by 50% after addition of the substrate (Fig. 2).

Affinity Measurement to hFAP by Fluorescence Polarization

Fluorescence polarization experiments were performed in 384-well plates (nonbinding, polystyrene, flat-bottom, black, high volume, 30 μL final volume). Stock solutions of proteins were serially diluted (1:2) with buffer (50 mM Tris, 100 mM NaCl, and 1 mM ethylenediaminetetraacetic acid, pH 7.4), whereas the final concentration of the binders (OncoFAP-fluorescein and BiOncoFAP-fluorescein) was kept constant at 10 nM. The fluorescence anisotropy was measured on a microtiter plate reader (Tecan Life Sciences). Experiments were performed in triplicate, and the mean anisotropy values were fitted using Prism y = bottom + (top − bottom)/$(1 + 10^{((\mathrm{LogIC50} - X)*\mathrm{HillSlope})})$. The data are reported in Supplemental Figure 2.

Affinity Measurement to hFAP by Enzyme-Linked Immunosorbent Assay (ELISA)

Recombinant hFAP (1 μM, 5 mL) was biotinylated with biotin-LC-*N*-hydroxysuccinimide (100 equivalents) by incubation at room temperature under gentle agitation in 50 mM 4-(2-hydroxyethyl)-1-piperazineethanesulfonic acid (HEPES; VWR) and 100 mM NaCl buffer (pH 7.4). After 2 h, biotinylated hFAP was purified via a PD-10 column and dialyzed overnight in HEPES buffer. The following day, a StreptaWell (Roche) (transparent 96-well plate) was incubated with biotinylated hFAP (100 nM, 100 μL/well) for 1 h at room temperature and washed with PBS (3 times, 200 μL/well). The protein was blocked by adding 4% milk in PBS (200 μL/well, 30 min at room temperature) and then washed with PBS (3 times, 200 μL/well). Immobilized hFAP was incubated for 30 min in the dark with serial dilutions of OncoFAP-fluorescein (compound 7) and BiOncoFAP-fluorescein (compound 8) and then washed with PBS (3 times, 200 μL/well). A solution of rabbit anti-fluorescein isothiocyanate antibody (1 μg/mL, product 4510-7804; Bio-Rad) in 2% milk-PBS was added to each well (100 μL/well) and incubated for an additional 30 min in the dark. The resulting complex was washed with PBS (3 times, 200 μL/well) and incubated for an additional 30 min with protein A-horseradish peroxidase (1 μg/mL in 2% milk-PBS, 100 μL/well). Each well was washed with PBS with 0.1% polysorbate (3 times, 200 μL/well) and PBS (3 times, 200 μL/well). The substrate (3,3′,5,5′-tetramethylbenzidine) was added (100 μL/well) and developed in the dark for 2 min. The reaction was stopped by adding 50 μL of 1 M sulfuric acid. The absorbance was measured at 450 nm (reference level, 620–650 nm) with a Spark multimode microplate reader (Tecan Life Sciences).

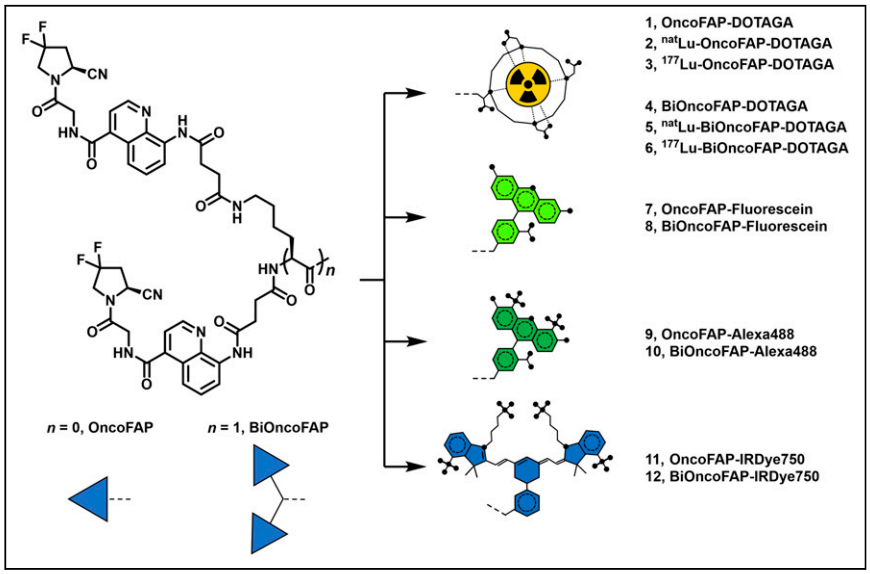

FIGURE 1. BiOncoFAP and OncoFAP and their DOTAGA, fluorescein, Alexa488, and IRDye750 conjugates.

Internalization Studies by Confocal Microscopy Analysis

SK-RC-52.hFAP and HT-1080.hFAP cells were seeded into 4-well coverslip chamber plates (Sarstedt, Inc.) at a density of 10^4 cells

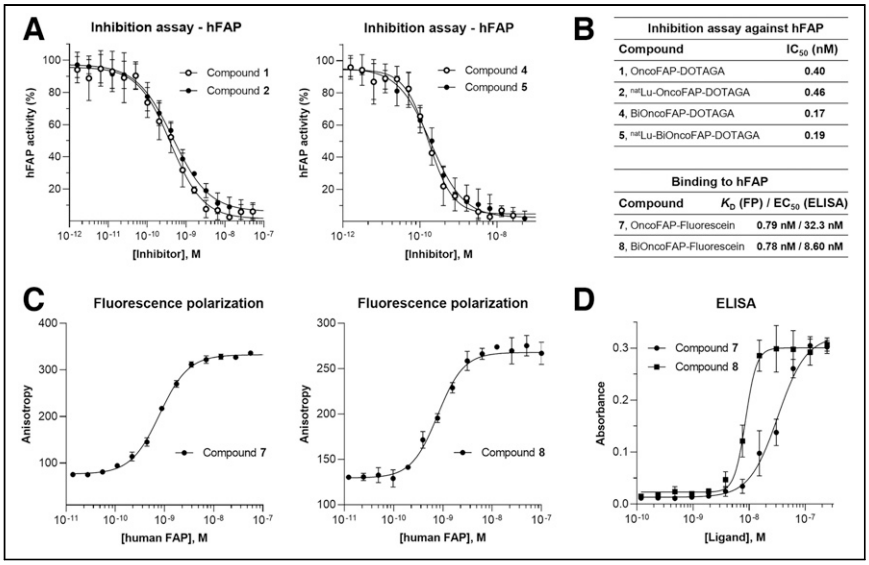

FIGURE 2. (A) Enzymatic assays performed with OncoFAP-DOTAGA (compound 1), BiOncoFAP-DOTAGA (compound 2), and their corresponding cold ^{nat}Lu-labeled derivatives (compounds 2 and 5). (B) Binding affinity and IC_{50} values for OncoFAP and BiOncoFAP derivatives toward hFAP. (C) Affinity measurement of OncoFAP-fluorescein (compound 7) and BiOncoFAP-fluorescein (compound 8) to recombinant hFAP by fluorescence polarization. Both compounds showed ultrahigh affinity for FAP target. (D) ELISA experiment on OncoFAP-fluorescein (compound 7) and BiOncoFAP-fluorescein (compound 8) against hFAP. FP = fluorescence polarization; K_D = affinity constant.

per well in RPMI-1640 medium (Gibco) or Dulbecco modified Eagle medium (Gibco), respectively (1 mL; Invitrogen) supplemented with 10% fetal bovine serum (Gibco), Antibiotic-Antimycotic (Gibco), and 10 mM HEPES. Cells were allowed to grow overnight under standard culture conditions. The culture medium was replaced with fresh medium containing the suitable Alexa488-conjugated probes (100 nM) and Hoechst 33342 nuclear dye (Invitrogen, 1 μg/mL). Colonies were randomly selected and imaged 30 min after incubation on an SP8 confocal microscope equipped with an acoustooptical beam splitterD (Leica Microsystems) (Fig. 3).

Animal Studies

All animal experiments were conducted in accordance with Swiss animal welfare laws and regulations under license ZH006/2021 granted by the Veterinäramt des Kantons Zürich.

Implantation of Subcutaneous Tumors

Tumor cells were grown to 80% confluence in Dulbecco modified Eagle medium or RPMI-1640 medium with 10% fetal bovine serum and 1% Antibiotic-Antimycotic and detached with trypsin-ethylenediaminetetraacetic acid, 0.05%. Tumor cells were resuspended in Hank's balanced salt solution medium. Aliquots of 5×10^6 cells (100 μL of suspension) were injected subcutaneously in the flank of female athymic BALB/c AnNRj-Foxn1 mice (6–8 wk old; Janvier).

Quantitative Biodistribution of ^{177}Lu-OncoFAP and ^{177}Lu-BiOncoFAP in Tumor-Bearing Mice

OncoFAP-DOTAGA (compound 1) and BiOncoFAP-DOTAGA (compound 4) were radiolabeled with ^{177}Lu (as described in the supplemental material). Tumors were allowed to grow to an average volume of 500 mm^3. Mice were randomized (4 or 5 per group) and injected intravenously with radiolabeled preparations of ^{177}Lu-OncoFAP and ^{177}Lu-BiOncoFAP (250 nmol/kg; 50 MBq/kg). The mice were euthanized by CO_2 asphyxiation at different time points (1, 4, 17, and 24 h) after the intravenous injection. Tumors, organs, and blood were harvested and weighed, and radioactivity was measured with a Packard Cobra γ-counter. Values are expressed as %ID/g ± SD (Fig. 4). The %ID/g in the tumors was corrected by tumor growth rate (*30*).

Therapy Studies with ^{177}Lu-OncoFAP and ^{177}Lu-BiOncoFAP in Tumor-Bearing Mice

The anticancer efficacy of ^{177}Lu-OncoFAP and ^{177}Lu-BiOncoFAP was assessed in athymic BALB/c AnNRj-Foxn1 mice bearing HT-1080.hFAP (right flank) and HT-1080.wt (wild type, left flank). ^{177}Lu-OncoFAP or ^{177}Lu-BiOncoFAP was intravenously administered at a dose of 250 nmol/kg, with 15 or 70 MBq/mouse (single administration, following the schedule indicated in Fig. 5). Therapy experiments started when the average volume of established tumors had reached 100–150 mm^3. The body weight of the animals and tumor volume were measured daily and recorded. Tumor dimensions were measured with an electronic caliper, and tumor volume was calculated with the formula (long side, mm) × (short side, mm) × (short side, mm) × 0.5. The animals were euthanized when one or more termination criteria indicated by the experimental license were reached (e.g., weight loss > 15%). Prism software was used for data analysis.

RESULTS

Preparation of OncoFAP and BiOncoFAP Conjugates

The dimeric ligand (BiOncoFAP-COOH, compound 13) was chemically synthesized exploiting L-lysine for the multimerization

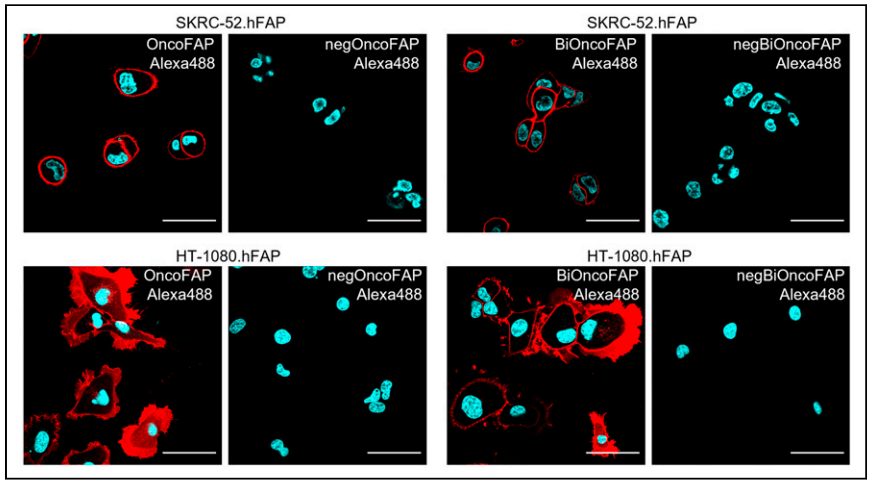

FIGURE 3. Confocal microscopy images after incubation of OncoFAP-Alexa488 (compound 9) and BiOncoFAP-Alexa488 (compound 10) with SK-RC-52.hFAP or HT-1080.hFAP. Red = fluorescein derivative staining; blue = Hoechst 33342 staining; scale bar = 50 μm.

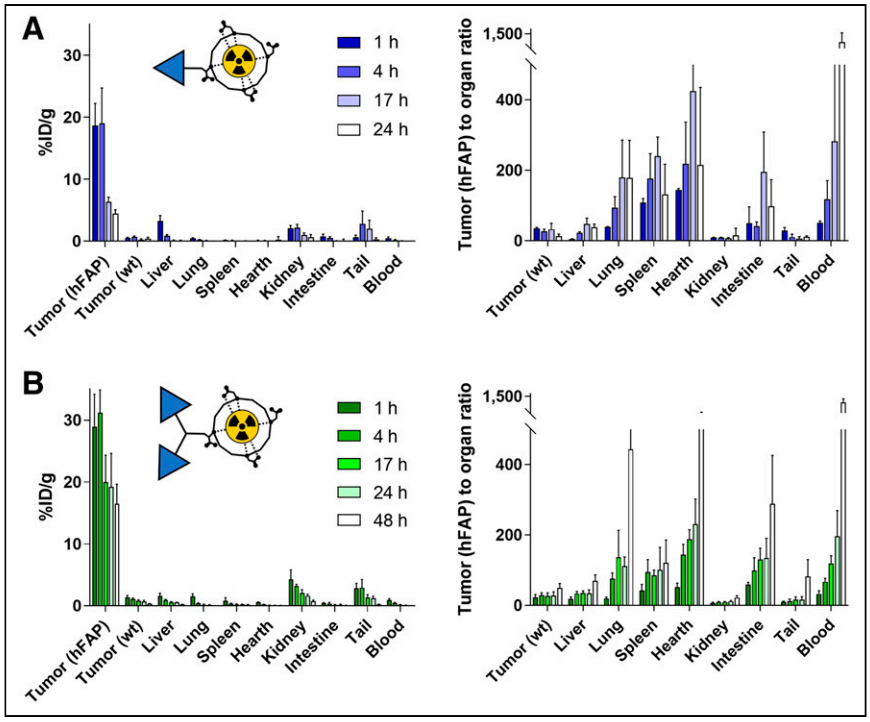

FIGURE 4. Quantitative in vivo biodistribution and tumor-to-organ ratio of ^{177}Lu-OncoFAP (compound 3) (A) and ^{177}Lu-BiOncoFAP (compound 6) (B) at different time points after intravenous administration (250 nmol/kg, 50 MBq/kg) in mice bearing HT-1080.wt and HT-1080.hFAP tumors.

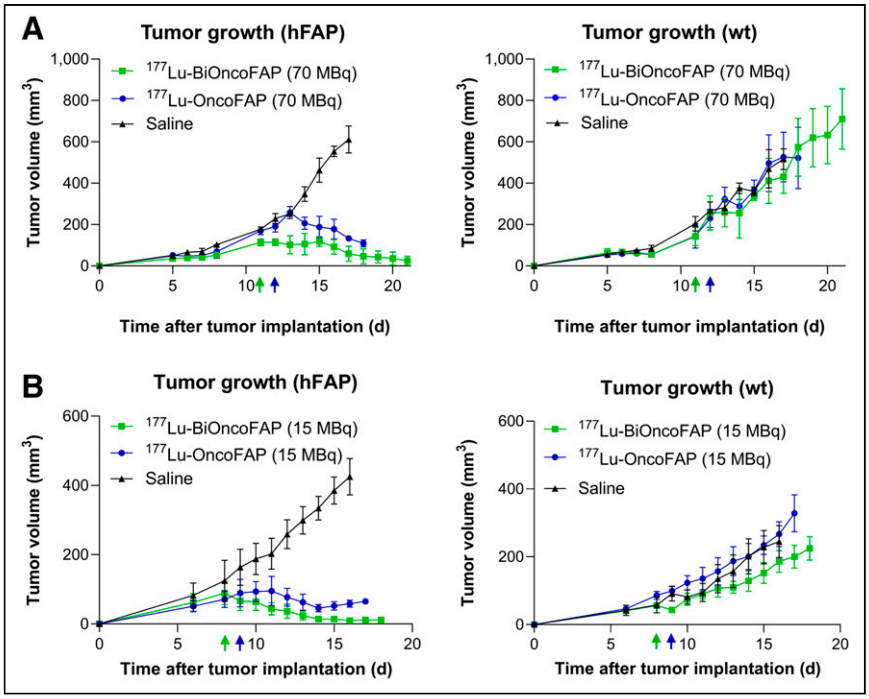

FIGURE 5. Therapeutic activity after single administration (250 nmol/kg) of ^{177}Lu-OncoFAP (compound 3) and ^{177}Lu-BiOncoFAP (compound 6) in BALB/c nu/nu-mice bearing HT-1080.hFAP tumor in right flank and HT-1080.wt tumor in left flank at dose of 70 MBq/mouse (A) or 15 MBq/mouse (B). Efficacy of different treatments was assessed by daily measurement of tumor volume (mm^3) after administration of different compounds. Data points represent mean tumor volume ± SEM.

of the OncoFAP targeting moiety. The free carboxylic acid served as a functional group for the conjugation of fluorophores (BiOncoFAP-fluorescein, compound 8; BiOncoFAP-Alexa488, compound 10; and BiOncoFAP-IRDye750, compound 12) and of DOTAGA chelator (compound 4). All compounds were produced in high yields and purities (supplemental material). Monovalent OncoFAP and the corresponding conjugates (OncoFAP-fluorescein, compound 7; OncoFAP-Alexa488, compound 9; and OncoFAP-IRDye750, compound 11) were synthesized following established procedures (*18*). The chemical structures of OncoFAP and BiOncoFAP derivatives are illustrated in Figure 1 and in the supplemental material. Radiolabeling of OncoFAP-DOTAGA (compound 1) and BiOncoFAP-DOTAGA (compound 4) with ^{177}Lu was achieved in high yield and purity (supplemental material). After radiolabeling, ^{177}Lu-OncoFAP and ^{177}Lu-BiOncoFAP retained the ability to form stable complexes with recombinant hFAP, as assessed by a PD-10 coelution experiment. Both compounds were highly hydrophilic, with experimental Log$D_{7.4}$ values of –4.02 ± 0.22 (n = 5) and –3.60 ± 0.31 (n = 5), respectively (supplemental material).

In Vitro Inhibition Assay Against hFAP

We evaluated the inhibitory activity of OncoFAP-DOTAGA (compound 1), BiOncoFAP-DOTAGA (compound 4), and their ^{nat}Lu cold-labeled derivatives (compounds 2 and 5, respectively) against hFAP. Compounds 4 and 5 displayed enhanced inhibitory activity against the target (IC_{50}, 168 and 192 pM, respectively), compared with their monovalent counterparts (OncoFAP-DOTAGA: IC_{50}, 399 pM; ^{nat}Lu-OncoFAP-DOTAGA: IC_{50}, 456 pM) (Figs. 2A and 2B).

Assessment of Binding Properties of BiOncoFAP to Soluble and Immobilized hFAP

To study the binding properties of OncoFAP and BiOncoFAP to soluble hFAP, we measured the affinity constant of the corresponding fluorescein conjugates (compound 8, OncoFAP-fluorescein, and compound 9, BiOncoFAP-fluorescein) in fluorescence polarization assays (Fig. 2C). Compounds 8 and 9 exhibited comparable subnanomolar affinity constants against hFAP (respectively, 795 and 781 pM). Moreover, both compounds were selective for FAP and did not bind to a set of nontarget proteins up to micromolar concentrations (Supplemental Fig. 2). Our data confirm that the

dimerization does not impair the affinity and selectivity of BiOncoFAP for its target. Then, we studied the binding affinity to hFAP immobilized on a solid support of the dimeric ligand. In a comparative ELISA, BiOncoFAP-fluorescein exhibited a lower affinity constant than OncoFAP-fluorescein (8.60 vs. 32.3 nM, respectively) (Figs. 2B and 2D).

Confocal Microscopy Analysis on Tumor Cells

Binding of BiOncoFAP to FAP-positive SK-RC-52 and HT-1080 cancer cells and internalization were assessed by confocal microscopy analysis using the corresponding Alexa-488 conjugate (compound 10). OncoFAP-Alexa488 (compound 9) was used in the same experiment as a positive control, whereas untargeted analogs were included as nonbinding negative controls (chemical structures are depicted in the supplemental material). OncoFAP and BiOncoFAP displayed comparable binding features on living tumor cells. Both compounds showed lack of internalization on FAP-positive SK-RC-52 cells, whereas high membrane trafficking was observed when compounds were incubated on HT-1080.hFAP cells (Fig. 3).

Stability Studies

The stability of cold-labeled ^{nat}Lu-BiOncoFAP-DOTAGA was assessed in human and mouse serum after incubation at 37°C for 24, 48, 72 and 120 h. The test compound exhibited a half-life longer than 5 d in all experimental conditions. No loss of lutetium (^{nat}Lu) from the DOTAGA chelator was detected (Supplemental Fig. 3).

Biodistribution of OncoFAP and BiOncoFAP in Tumor-Bearing Mice

The qualitative biodistribution of OncoFAP and BiOncoFAP was assessed in tumor-bearing mice using a near-infrared fluorophore (IRDye750) as a detection agent. Macroscopic imaging of mice implanted with SK-RC-52.hFAP (right flank) and SK-RC-52.wt (left flank) tumors revealed that both OncoFAP-IRDye750 (compound 11) and BiOncoFAP-IRDye750 (compound 12) selectively accumulated in FAP-positive tumors (Supplemental Figs. 4 and 5). Interestingly, the BiOncoFAP-IRDye750 conjugate exhibited a longer residence time at the site of disease. Encouraged by these results, we studied the quantitative biodistribution of ^{177}Lu-BiOncoFAP in athymic BALB/c mice bearing HT-1080.hFAP (right flank) and HT-1080.wt (left flank) tumors. A direct comparison with ^{177}Lu-OncoFAP was included in the experiment (Fig. 4). Both compounds accumulated selectively in FAP-positive tumors shortly after intravenous administration. The dimeric ^{177}Lu-BiOncoFAP product exhibited a more stable and prolonged tumor uptake than its monovalent counterpart (~20 vs. ~4 %ID/g, 24 h after systemic administration). Notably, ^{177}Lu-BiOncoFAP did not show significant uptake in healthy organs, with a favorable tumor-to-organ ratio (e.g., 22-to-1 tumor-to-kidney ratio and 70-to-1 tumor-to-liver ratio, at the 48-h time point) (Supplemental Tables 1–4).

In Vitro Cell Binding and Efflux Assays with ^{177}Lu-OncoFAP and ^{177}Lu-BiOncoFAP on HT-1080.hFAP Cells

Cell binding of ^{177}Lu-OncoFAP and ^{177}Lu-BiOncoFAP was assessed on HT-1080.hFAP cells, following literature procedures (*29*). Both compounds showed high binding properties toward the FAP-positive cell line. The binding was efficiently antagonized by a large excess of cold competitors (OncoFAP-DOTAGA or BiOncoFAP-DOTAGA) (Supplemental Fig. 6A). Cell efflux experiments revealed a longer half-life for ^{177}Lu-BiOncoFAP (~36 h) than for the monovalent counterpart (~18 h) (Supplemental Fig. 6B).

Therapy Study

The therapeutic efficacy of ^{177}Lu-OncoFAP and of ^{177}Lu-BiOncoFAP was assessed in mice bearing HT-1080.hFAP tumors on the right flank and HT-1080.wt tumors on the left flank (Fig. 5; Supplemental Fig. 7). Systemic administration of both compounds at therapeutic doses (15 or 70 MBq/mouse, 250 nmol/kg) resulted in selective and potent anticancer activity against the growth of HT-1080.hFAP as compared with mice injected with saline. The most active compound in our therapy studies was ^{177}Lu-BiOncoFAP. Tumor growth of FAP-negative lesions (HT-1080.wt) was not influenced by the treatment with ^{177}Lu-OncoFAP or with ^{177}Lu-BiOncoFAP. No significant change in mouse body weight was detected with either the 15- or the 70-MBq dose (Supplemental Fig. 8).

DISCUSSION

FAP-targeting radiopharmaceuticals may revolutionize the field of radioligand imaging of cancer because of their applicability to many types of malignancies and their excellent tumor selectivity, which has already been proven at the clinical level (*12,13,19*). Other SMRC products—^{177}Lu-PSMA-617 and ^{177}Lu-DOTATATE—are limited to certain specific cancer indications and may be taken up by certain normal organ structures (*31,32*). FAP is expressed mainly in the stroma of solid malignancies and on the tumor cell surface of mesenchymal tumors, thus adding a new element of differentiation compared with previously established targeting platforms, based on somatostatin receptor type 2 and PSMA (*12,13,16,17*), which are expressed on the surface of cancer cells. In this context, accurate selection of the radionuclide payload is crucial to the success of FAP-targeting radiotherapy. Although α-emitters are characterized by a short range, typically more than 100 μm (*33*) which may be insufficient, the use of a β-emitter radionuclide such as ^{177}Lu (pathlength of ~1.5 mm) (*33*) may enable the killing of stromal cells and surrounding tumor cells (*34,35*).

Sustained accumulation of SMRCs in tumors is fundamental to the effective delivery of high radiation doses over time at the site of disease and, therefore, to the success of the treatment. Among different approaches used in the past, dimerization of high-affinity ligands has been proposed as a strategy to enhance residence time in antigen-positive structures (i.e., in FAP-positive tumors) (*23,36–39*). Dimeric ligands present higher chances of rebinding to their target, with slower off-rates than are seen with their monovalent counterparts (*40*). However, an increase in the binding valency typically leads to higher uptake in healthy tissues (*21,38,39*). To the best of our knowledge, only 3 dimeric FAP-targeting radionuclides—DOTA/DOTAGA.(SA.FAPi)$_2$ (*41,42*), DOTA-2P(FAPi)$_2$ (*21*), and ND-bisFAPI (*29*)—have recently been described. Although preclinical biodistribution data are not available for DOTA/DOTAGA.(SA.FAPi)$_2$, DOTA-2P(FAPi)$_2$ was extensively characterized in an HCC-PDX-1 mouse model. Despite its slightly increased tumor uptake compared with the monovalent FAPI-46 (~9% vs. ~4 %ID/g 1 h after injection), the dimeric ligand presents low tumor-to-organ ratios both at 1 h and 4 h, with a particular liability for the kidney (~1.2-to-1 and ~1.5-to-1 tumor-to-kidney ratios, respectively) (*21*). Similarly, ND-bisFAPI exhibited increased tumor uptake in A549-FAP xenografts, with low tumor-to-organ ratios at all investigated time points (i.e., from 1 to 72 h after systemic administration) (*29*). BiOncoFAP, the novel homodimeric FAP-targeting small organic ligand described in this article, shows specific and persistent tumor uptake (~30 %ID/g 1 h after injection and ~16 %ID/g at 48 h after injection) in HT-1080.hFAP tumor–bearing mice. Remarkably,

^{177}Lu-BiOncoFAP presents a clean preclinical biodistribution profile with high tumor-to-organ ratios even at early time points (e.g., ∼7-to-1 and ∼10-to-1 tumor-to-kidney ratio and ∼20-to-1 and ∼34-to-1 tumor-to-liver ratio at the 1 and 4 h time points, respectively).

The in vivo anticancer activity of ^{177}Lu-FAPI-46 (β-emitter) and ^{225}Ac-FAPI-46 (α-emitter) has recently been evaluated in PANC-1 tumor–bearing mice, a xenograft model of pancreatic cancer characterized by high stromal expression of FAP (*35*). Both products showed only limited tumor growth suppression even at the highest dose (i.e., 30 kBq/mouse for ^{225}Ac-FAPI-46 and 30 MBq/mouse for ^{177}Lu-FAPI-46).

Collectively, our biodistribution and therapy results show that both ^{177}Lu-OncoFAP and ^{177}Lu-BiOncoFAP are able to efficiently localize at the tumor site and produce a potent anticancer effect in mice bearing subcutaneous FAP-positive tumors, after a single administration at a dose of 70 MBq (∼2 mCi)/mouse or 15 MBq (∼0.4 mCi)/mouse. Compared with the monomeric ^{177}Lu-OncoFAP, our new bivalent ^{177}Lu-BiOncoFAP displayed an enhanced in vivo antitumor activity. As expected, lack of tumor suppression was observed for the FAP-negative tumors (HT-1080.wt), which were used as an internal control to appreciate the specificity of OncoFAP-based theranostic products toward FAP-positive solid lesions. In this article, we have presented the favorable biodistribution profile and therapeutic efficacy of ^{177}Lu-OncoFAP and ^{177}Lu-BiOncoFAP obtained in xenograft models with stable, homogeneous expression of hFAP on the surface of tumor cells. Further investigations in tumor models with a stromal pattern of FAP expression (e.g., patient-derived xenografts) will be of pivotal importance to predict the therapeutic performance of OncoFAP and BiOncoFAP-based therapeutics in the view of future clinical studies.

Considering the exquisite selectivity for cancer lesions and pantumoral properties of FAP-targeting radioligand therapeutics, this new class of radiopharmaceutical products may represent a breakthrough in cancer therapy (*12*). Interim reports on the efficacy of the FAP-targeting peptides and small organic ligands developed so far have shown this therapeutic strategy to have limitations (*26,43*). Escalation of the dose of radiolabeled FAP-targeting peptides is limited by their intrinsically high kidney uptake at late time points (*43–45*). Therapy with small organic ligands based on FAPI-46 may be limited by their short residence time in the tumor (*26,46*). We have developed ^{177}Lu-BiOncoFAP, a new radioligand therapeutic product with prolonged in vivo tumor uptake and highly favorable tumor-to-kidney ratios. Future clinical studies on a basket of indications will provide clarity on the therapeutic efficacy of this novel FAP-targeting product.

CONCLUSION

^{177}Lu-BiOncoFAP is a promising FAP-targeting SMRC product for tumor therapy. This novel bivalent FAP-targeting compound binds its target with high affinity and shows a long residence time in tumor lesions, with favorable tumor-to-organ ratios. Once administered at therapeutic doses, ^{177}Lu-BiOncoFAP potently inhibits growth of FAP-positive tumors in mice. Our data support clinical development of ^{177}Lu-BiOncoFAP in the frame of targeted radioligand therapy.

DISCLOSURE

Dario Neri is a cofounder and shareholder of Philogen (http://www.philogen.com/en/), a Swiss–Italian Biotech company that operates in the field of ligand-based pharmacodelivery. Andrea Galbiati, Aureliano Zana, Matilde Bocci, Jacopo Millul, Abdullah Elsayed, Jacqueline Mock, and Samuele Cazzamalli are employees of Philochem AG, the daughter company of Philogen that owns and has patented OncoFAP (PCT/EP2021/053494) and BiOncoFAP (PCT/EP2022/053404). No other potential conflict of interest relevant to this article was reported.

ACKNOWLEDGMENTS

We thank Ettore Gilardoni for performing an exact mass analysis of compounds presented in this article, and Frederik Peissert and Luca Prati for their support with small-molecule ELISA experiments.

KEY POINTS

QUESTION: Does ligand dimerization enhance the tumor retention time and therapeutic potential of FAP-targeting radioconjugates?

PERTINENT FINDINGS: Compared with its OncoFAP monovalent counterpart, dimeric ^{177}Lu-BiOncoFAP shows higher and longer tumor uptake in tumor-bearing mice. ^{177}Lu-BiOncoFAP displays a potent in vivo anticancer effect in preclinical murine models.

IMPLICATIONS FOR PATIENT CARE: The prolonged tumor uptake of ^{177}Lu-BiOncoFAP supports clinical development for the targeted radioligand therapy of multiple FAP-positive cancer lesions.

REFERENCES

1. Dal Corso A. Targeted small-molecule conjugates: the future is now. *ChemBioChem.* 2020;21:3321–3322.
2. Sun X, Li Y, Liu T, Li Z, Zhang X, Chen X. Peptide-based imaging agents for cancer detection. *Adv Drug Deliv Rev.* 2017;110–111:38–51.
3. Siva S, Udovicich C, Tran B, Zargar H, Murphy DG, Hofman MS. Expanding the role of small-molecule PSMA ligands beyond PET staging of prostate cancer. *Nat Rev Urol.* 2020;17:107–118.
4. Ballinger JR. Theranostic radiopharmaceuticals: established agents in current use. *Br J Radiol.* 2018;91:20170969.
5. Turner JH. An introduction to the clinical practice of theranostics in oncology. *Br J Radiol.* 2018;91:20180440.
6. Lenzo NP, Meyrick D, Turner JH. Review of gallium-68 PSMA PET/CT imaging in the management of prostate cancer. *Diagnostics (Basel).* 2018;8:16.
7. Turner JH. Recent advances in theranostics and challenges for the future. *Br J Radiol.* 2018;91:20170893.
8. Herrero Álvarez N, Bauer D, Hernández-Gil J, Lewis JS. Recent advances in radiometals for combined imaging and therapy in cancer. *ChemMedChem.* 2021;16:2909–2941.
9. Hennrich U, Kopka K. Lutathera®: the first FDA- and EMA-approved radiopharmaceutical for peptide receptor radionuclide therapy. *Pharmaceuticals (Basel).* 2019;12:114.
10. Strosberg J, El-Haddad G, Wolin E, et al. Phase 3 trial of ^{177}Lu-DOTATATE for midgut neuroendocrine tumours. *N Engl J Med.* 2017;376:125–135.
11. Sartor O, de Bono J, Chi KN, et al. Lutetium-177–PSMA-617 for metastatic castration-resistant prostate cancer. *N Engl J Med.* 2021;385:1091–1103.
12. Calais J. FAP: the next billion dollar nuclear theranostics target? *J Nucl Med.* 2020;61:163–165.
13. Kratochwil C, Flechsig P, Lindner T, et al. ^{68}Ga-FAPI PET/CT: tracer uptake in 28 different kinds of cancer. *J Nucl Med.* 2019;60:801–805.
14. Backhaus P, Burg M, Roll W, et al. A new horizon for breast cancer staging: first evidence from simultaneous PET-MRI targeting the fibroblast activating protein (FAP) [abstract]. *Nuklearmedizin.* 2021;60:L10.
15. Backhaus P, Burg MC, Roll W, et al. Simultaneous FAPI PET/MRI targeting the fibroblast-activation protein for breast cancer. *Radiology.* 2022;302:39–47.
16. Lo A, Wang LCS, Scholler J, et al. Tumour-promoting desmoplasia is disrupted by depleting FAP-expressing stromal cells. *Cancer Res.* 2015;75:2800–2810.
17. Mona CE, Benz MR, Hikmat F, et al. Correlation of ^{68}Ga-FAPi-46 PET biodistribution with FAP expression by immunohistochemistry in patients with solid

cancers: interim analysis of a prospective translational exploratory study. *J Nucl Med.* 2022;63:1021–1026.
18. Millul J, Bassi G, Mock J, et al. An ultra-high-affinity small organic ligand of fibroblast activation protein for tumour-targeting applications. *Proc Natl Acad Sci USA.* 2021;118:e2101852118.
19. Backhaus P, Gierse F, Burg MC, et al. Translational imaging of the fibroblast activation protein (FAP) using the new ligand [^{68}Ga]Ga-OncoFAP-DOTAGA. *Eur J Nucl Med Mol Imaging.* 2022;49:1822–1832.
20. Mansi R, Fani M. Radiolabeled peptides for cancer imaging and therapy: from bench-to-bedside. *Chimia (Aarau).* 2021;75:500–504.
21. Zhao L, Niu B, Fang J, et al. Synthesis, preclinical evaluation, and a pilot clinical PET imaging study of ^{68}Ga-labeled FAPI dimer. *J Nucl Med.* 2022;63:862–868.
22. Jones W, Griffiths K, Barata PC, Paller CJ. PSMA theranostics: review of the current status of PSMA-targeted imaging and radioligand therapy. *Cancers (Basel).* 2020;12:1367.
23. Schäfer M, Bauder-Wüst U, Leotta K, et al. A dimerized urea-based inhibitor of the prostate-specific membrane antigen for ^{68}Ga-PET imaging of prostate cancer. *EJNMMI Res.* 2012;2:23.
24. Gupta SK, Singla S, Thakral P, Bal CS. Dosimetric analyses of kidneys, liver, spleen, pituitary gland, and neuroendocrine tumours of patients treated with ^{177}Lu-DOTATATE. *Clin Nucl Med.* 2013;38:188–194.
25. Schuchardt C, Zhang J, Kulkarni HR, Chen X, Müller D, Baum RP. Prostate-specific membrane antigen radioligand therapy using ^{177}Lu-PSMA I&T and ^{177}Lu-PSMA-617 in patients with metastatic castration-resistant prostate cancer: comparison of safety, biodistribution, and dosimetry. *J Nucl Med.* 2022;63:1199–1207.
26. Kaghazchi F, Aghdam RA, Haghighi S, Vali R, Adinehpour Z. ^{177}Lu-FAPI therapy in a patient with end-stage metastatic pancreatic adenocarcinoma. *Clin Nucl Med.* 2022;47:e243–e245.
27. Meyer C, Dahlbom M, Lindner T, et al. Radiation dosimetry and biodistribution of ^{68}Ga-FAPI-46 PET imaging in cancer patients. *J Nucl Med.* 2020;61:1171–1177.
28. Loktev A, Lindner T, Burger EM, et al. Development of fibroblast activation protein–targeted radiotracers with improved tumour retention. *J Nucl Med.* 2019;60:1421–1429.
29. Li H, Ye S, Li L, et al. ^{18}F- or ^{177}Lu-labeled bivalent ligand of fibroblast activation protein with high tumor uptake and retention. *Eur J Nucl Med Mol Imaging.* 2022;49:2705–2715.
30. Tarli L, Balza E, Viti F, et al. A high-affinity human antibody that targets tumoural blood vessels. *Blood.* 1999;94:192–198.
31. Tönnesmann R, Meyer PT, Eder M, Baranski AC. [^{177}Lu]Lu-PSMA-617 salivary gland uptake characterized by quantitative in vitro autoradiography. *Pharmaceuticals (Basel).* 2019;12:18.
32. Geenen L, Nonnekens J, Konijnenberg M, Baatout S, De Jong M, Aerts A. Overcoming nephrotoxicity in peptide receptor radionuclide therapy using [^{177}Lu]Lu-DOTA-TATE for the treatment of neuroendocrine tumours. *Nucl Med Biol.* 2021;102–103:1–11.
33. Navalkissoor S, Grossman A. Targeted alpha particle therapy for neuroendocrine tumours: the next generation of peptide receptor radionuclide therapy. *Neuroendocrinology.* 2019;108:256–264.
34. Frey K, Neri D. Antibody-based targeting of tumor vasculature and stroma. In: *Tumor-Associated Fibroblasts and Their Matrix.* Springer; 2011:419–450.
35. Liu Y, Watabe T, Kaneda-Nakashima K, et al. Fibroblast activation protein targeted therapy using [^{177}Lu]FAPI-46 compared with [^{225}Ac]FAPI-46 in a pancreatic cancer model. *Eur J Nucl Med Mol Imaging.* 2022;49:871–880.
36. Gaertner FC, Kessler H, Wester HJ, Schwaiger M, Beer AJ. Radiolabelled RGD peptides for imaging and therapy. *Eur J Nucl Med Mol Imaging.* 2012;39(suppl):S126–S138.
37. Liu S. Radiolabeled cyclic RGD peptides as integrin αvβ3-targeted radiotracers: maximizing binding affinity via bivalency. *Bioconjug Chem.* 2009;20:2199–2213.
38. Krall N, Pretto F, Neri D. A bivalent small molecule-drug conjugate directed against carbonic anhydrase IX can elicit complete tumour regression in mice. *Chem Sci.* 2014;5:3640–3644.
39. Liu S. Radiolabeled multimeric cyclic RGD peptides as integrin αvβ3 targeted radiotracers for tumour imaging. *Mol Pharm.* 2006;3:472–487.
40. Chittasupho C. Multivalent ligand: design principle for targeted therapeutic delivery approach. *Ther Deliv.* 2012;3:1171–1187.
41. Ballal S, Yadav MP, Moon ES, et al. First-in-human results on the biodistribution, pharmacokinetics, and dosimetry of [^{177}Lu]Lu-DOTA.SA.FAPi and [^{177}Lu]Lu-DOTAGA.(SA.FAPi)2. *Pharmaceuticals (Basel).* 2021;14:1212.
42. Qin C, Song Y, Cai W, Lan X. Dimeric FAPI with potential for tumour theranostics. *Am J Nucl Med Mol Imaging.* 2021;11:537–541.
43. Baum RP, Schuchardt C, Singh A, et al. Feasibility, biodistribution, and preliminary dosimetry in peptide-targeted radionuclide therapy of diverse adenocarcinomas using ^{177}Lu-FAP-2286: first-in-humans results. *J Nucl Med.* 2022;63:415–423.
44. Zhao L, Shang Q, Wu H, Lin Q. Fibroblast activation protein-based theranostics in cancer research: a state-of-the-art review. *Theranostics.* 2022;12:1557–1569.
45. Nishio M, Okamoto I, Murakami H, et al. Preclinical evaluation of FAP-2286, a peptide-targeted radionuclide therapy (PTRT) to fibroblast activation protein alpha (FAP) [abstract]. *Ann Oncol.* 2020;31(suppl 4):S488.
46. Assadi M, Rekabpour SJ, Jafari E, et al. Feasibility and therapeutic potential of ^{177}Lu-fibroblast activation protein inhibitor-46 for patients with relapsed or refractory cancers: a preliminary study. *Clin Nucl Med.* 2021;46:e523–e530.